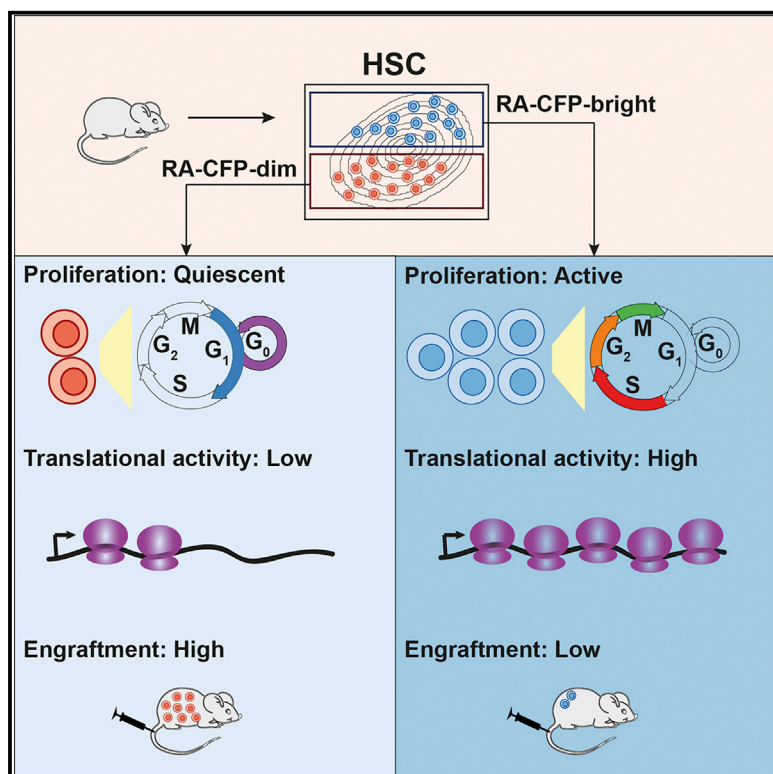


Differences in Cell Cycle Status Underlie Transcriptional Heterogeneity in the HSC Compartment

Graphical Abstract



Highlights

- The RA-CFP reporter can be used for sub-fractionation of HSCs
- RA-CFP-dim HSCs are endowed with superior engraftment potential
- RA-CFP-dim HSC are slow cycling and enriched in label-retaining cells
- Transcriptional heterogeneity within HSCs is associated with cell cycle differences

Authors

Felicia Kathrine Bratt Lauridsen,
Tanja Lyholm Jensen, Nicolas Rapin, ...,
Palle Serup, Ido Amit, Bo Torben Porse

Correspondence

bo.porse@finsenlab.dk

In Brief

HSCs are considered a functional heterogeneous population. Lauridsen et al. use scRNA-seq to demonstrate that most transcriptional heterogeneity within the HSC compartment is associated with differences in cell cycle status. They further use an RA-CFP reporter mouse line to isolate slow-cycling HSCs characterized by superior engraftment potential.

Data and Software Availability

GSE108155



Differences in Cell Cycle Status Underlie Transcriptional Heterogeneity in the HSC Compartment

Felicia Kathrine Bratt Lauridsen,^{1,2,3,5} Tanja Lyholm Jensen,^{1,2,3,5} Nicolas Rapin,^{1,2,3,5} Derya Aslan,^{1,2,3}

Anna Sofia Wilhelmsson,^{1,2,3} Sachin Pundhir,^{1,2,3} Matilda Rehn,^{1,2,3} Franziska Paul,⁴ Amir Giladi,⁴

Marie Sigurd Hasemann,^{1,2,3} Palle Serup,³ Ido Amit,⁴ and Bo Torben Porse^{1,2,3,6,*}

¹The Finsen Laboratory, Rigshospitalet, Faculty of Health Sciences, University of Copenhagen, 2200 Copenhagen, Denmark

²Biotech Research and Innovation Center (BRIC), University of Copenhagen, 2200 Copenhagen, Denmark

³Novo Nordisk Foundation Center for Stem Cell Biology, DanStem, Faculty of Health Sciences, University of Copenhagen, Denmark

⁴Weizmann Institute of Science, Rehovot 7610001, Israel

⁵These authors contributed equally

⁶Lead Contact

*Correspondence: bo.porse@finsenlab.dk

<https://doi.org/10.1016/j.celrep.2018.06.057>

SUMMARY

Hematopoietic stem cells (HSCs) are considered a heterogeneous cell population. To further resolve the HSC compartment, we characterized a retinoic acid (RA) reporter mouse line. Sub-fractionation of the HSC compartment in RA-CFP reporter mice demonstrated that RA-CFP-dim HSCs were largely non-proliferative and displayed superior engraftment potential in comparison with RA-CFP-bright HSCs. Gene expression analysis demonstrated higher expression of RA-target genes in RA-CFP-dim HSCs, in contrast to the RA-CFP reporter expression, but both RA-CFP-dim and RA-CFP-bright HSCs responded efficiently to RA *in vitro*. Single-cell RNA sequencing (RNA-seq) of >1,200 HSCs showed that differences in cell cycle activity constituted the main driver of transcriptional heterogeneity in HSCs. Moreover, further analysis of the single-cell RNA-seq data revealed that stochastic low-level expression of distinct lineage-affiliated transcriptional programs is a common feature of HSCs. Collectively, this work demonstrates the utility of the RA-CFP reporter line as a tool for the isolation of superior HSCs.

INTRODUCTION

The bone marrow (BM) is one of the most proliferative tissues found in the body, with billions of cells produced every day to replace damaged, exhausted, and dead cells. This massive proliferative expansion is undertaken mainly by hematopoietic progenitor cells (Passegué et al., 2005). Historically, it has been argued that the hematopoietic stem cells (HSCs) are the critical cells responsible for maintaining the hematopoietic system. This is based on the fact that these are the only cells which show long-

term engraftment in *in vivo* transplantation assays (Dykstra et al., 2007). However, recent studies based on lineage-tracing approaches have indicated a minor role for HSCs during steady-state hematopoiesis and instead implicated multipotent progenitors as the major source of mature cells (Busch et al., 2015; Sun et al., 2014). This notion was recently challenged, suggesting that HSCs are indeed the main contributor to hematopoietic output even in steady state (Sawai et al., 2016).

Label retention studies have shown that a subset of HSCs is highly quiescent and likely proliferate only four or five times during the lifespan of a mouse (Bernitz et al., 2016; Wilson et al., 2008). Thus, it has been hypothesized that the proliferative status of HSCs is important for their functional capacity and that proliferating HSC subsets display diminished reconstitution potential in transplantation experiments (Bowie et al., 2006; Nygren et al., 2006). It has even been suggested that when HSCs exit dormancy and undergo cell division, they are not able to return to full dormancy and are therefore destined for elimination (Qu et al., 2014).

In addition to showing heterogeneity in terms of cell cycle status, numerous publications have addressed the functional heterogeneity of HSCs in relation to their lineage bias. For instance, using single-cell transplantation assays, the existence of lymphoid-deficient α -HSCs (responsible for producing cells of mainly the myeloid lineage) and balanced β -HSCs (having equal output of myeloid and lymphoid cells) has been demonstrated (Dykstra et al., 2007). It was hypothesized that the α -HSCs constituted the most immature HSC population because these could give rise to β -HSCs in secondary transplants, whereas β -HSCs did not give rise to α -HSCs. Recently, in a study using a transgenic murine model with GFP inserted into the *Vwf* locus, evidence was presented suggesting that a platelet-biased HSC population reside at the apex of the hematopoietic system and is able to give rise to more myeloid-biased HSCs, possibly resembling the previously described lymphoid-deficient α -HSC population (Sanjuan-Pla et al., 2013).

The issue of transcriptional lineage priming was first investigated almost 20 years ago in a primitive cell line retaining the



capability of multilineage differentiation (Hu et al., 1997). Using single-cell RT-qPCR, the authors demonstrated the co-expression of the erythroid globin gene and the granulocytic gene encoding myeloperoxidase, arguing for low-level expression of distinct lineage genes prior to definite lineage commitment. Recently, single-cell RNA sequencing (scRNA-seq) has emerged as a powerful tool to dissect subpopulations within tissues (Paul et al., 2015). Although this technique has been applied to HSCs, spurious expression of distinct lineage markers has not been reported in HSCs. Instead, evidence for the existence of discrete clusters with predominant expression of specific lineage genes has been presented (Tsang et al., 2015). In this early work, the main driver of gene expression variance in both young and aged HSCs is cell cycle-associated genes (Kowalczyk et al., 2015). Other than cell cycle, it has not been possible to dissect further the HSC population into discrete subsets. This is despite the fact that not all HSCs are able to give rise to progeny when transplanted as single cells using stringent gating strategies and that transplantation assays do show lineage bias of individually transplanted HSCs (Dykstra et al., 2007).

These previous studies emphasize the importance of maintaining HSC quiescence and reveal a significant heterogeneity within the HSC compartment (at least with respect to cycling status). Several factors have been shown to be essential for HSC quiescence, and numerous studies have highlighted the HSC niche as an important player in maintaining the quiescent nature of long-term HSCs (LT-HSCs) (Morrison and Scadden, 2014). Multiple extracellular signals exert their effect on cell function by regulating gene transcription. One such pathway is the RA signaling pathway, which has been reported to act both in paracrine and autocrine manners (Cunningham and Duester, 2015). Within the hematopoietic system, RA signaling through RARA is best known for its differentiation-inducing effects on myeloid progenitors (Purton et al., 1999). For murine HSCs, it has been suggested that RA enhances self-renewal via signaling through RARG, as RA treatment of murine hematopoietic progenitors increases the repopulation ability of these cells and limits culture-induced differentiation (Purton et al., 2000, 2006). Recently, RA signaling was also shown to be important for HSC dormancy (Cabezas-Wallscheid et al., 2017). However, studies using HSPCs from either cord blood or adult human BM suggest an opposite role of RA signaling in the human system (Chute et al., 2006). Whether these discrepancies highlight an actual difference between the murine and the human system, or whether they are related to the experimental setup, is yet to be determined.

In the present study, we explored the possibility of using an RA-CFP reporter mouse line to elucidate HSC heterogeneity and efficiently isolate HSC subpopulations.

RESULTS

Robust Retinoic Acid Reporter Expression Marks Specific Hematopoietic Subsets

We set out to explore whether we could resolve HSC heterogeneity using murine reporter models for the bone morpho-

genic protein (BMP), wingless-type MMTV integration site family member (Wnt), and retinoic acid (RA) signaling pathways. These models were generated previously by replacing portions of the Rosa26 promoter with pathway-specific response elements inserted upstream of a cerulean fluorescent protein (CFP) cDNA. Work in embryonic stem cells has shown these reporters to be highly sensitive and specific for their respective ligands (Serup et al., 2012). Within the murine BM we only detected robust reporter expression in the DR5-TA-RA-CFP model reporting on RA signaling (hereinafter referred to as RA-CFP) (Figures 1A and 1B). Across the hematopoietic system, we detected variable RA-CFP expression patterns, with the HSC compartment (defined as LSK, CD150⁺, CD48⁻) displaying a relatively narrow intermediate level of expression (Figure 1B). When analyzing the hematopoietic progenitor compartments in further detail, we observed the highest reporter expression in granulocytic-macrophage progenitors (GMPs), in line with RA promoting the differentiation of myeloid progenitors (Purton et al., 1999) (Figures 1C and S1A). Interestingly, we also observed high reporter levels in erythroid progenitors (pre-CFU-Es, CFU-Es, and MkP), suggesting that in addition to its previously reported cell-extrinsic role during erythropoiesis, RA signaling may also regulate this process via cell-intrinsic mechanisms (Dewamitta et al., 2014). In mature populations, both Ter119⁺ erythroid and CD8⁺ T-lymphoid cells separated clearly into RA-CFP-positive and RA-CFP-negative populations (Figures S1B and S1C). This suggests a potential role for RA signaling in different T cell and erythroid subsets.

To confirm the RA sensitivity of our reporter model in the hematopoietic system, we sorted cKit⁺ cells with low and narrow RA-CFP expression and placed them in culture with RA in the presence and absence of the pan-RA receptor inverse agonist BMS493. RA rapidly induced CFP mRNA and protein expression in a dose-dependent manner (Figures 1D, S1D, and S1E). This induction was blocked by addition of BMS493, demonstrating that CFP expression is indeed responsive to RA signaling. Addition of BMS493 alone did not lower the reporter signal compared with DMSO, arguing against ongoing reporter activity in this setting (Figure S1F).

In summary, we identified distinct expression of RA-CFP across different hematopoietic populations, with HSCs showing a tight intermediate expression. Additionally, RA-CFP levels in cultured hematopoietic progenitor cells responded to RA addition in a dose-dependent manner.

RA-CFP Levels Predict HSC Engraftment

In order to evaluate whether there was a functional difference in HSCs with varying CFP levels, we carried out transplantation assays and monitored recipients for 16 weeks. HSCs were isolated on the basis of their CFP fluorescence into two subpopulations: RA-CFP dim (lowest ~20% CFP expression) and RA-CFP bright (highest ~20% CFP expression). One hundred HSCs (RA-CFP dim, RA-CFP bright, or unfractionated; all CD45.2) were subsequently transplanted along with 400,000 CD45.1 whole BM (wBM) cells into lethally irradiated recipient mice (CD45.1) (Figure 2A). We observed an inverse correlation between the RA-CFP fluorescence in HSCs and their

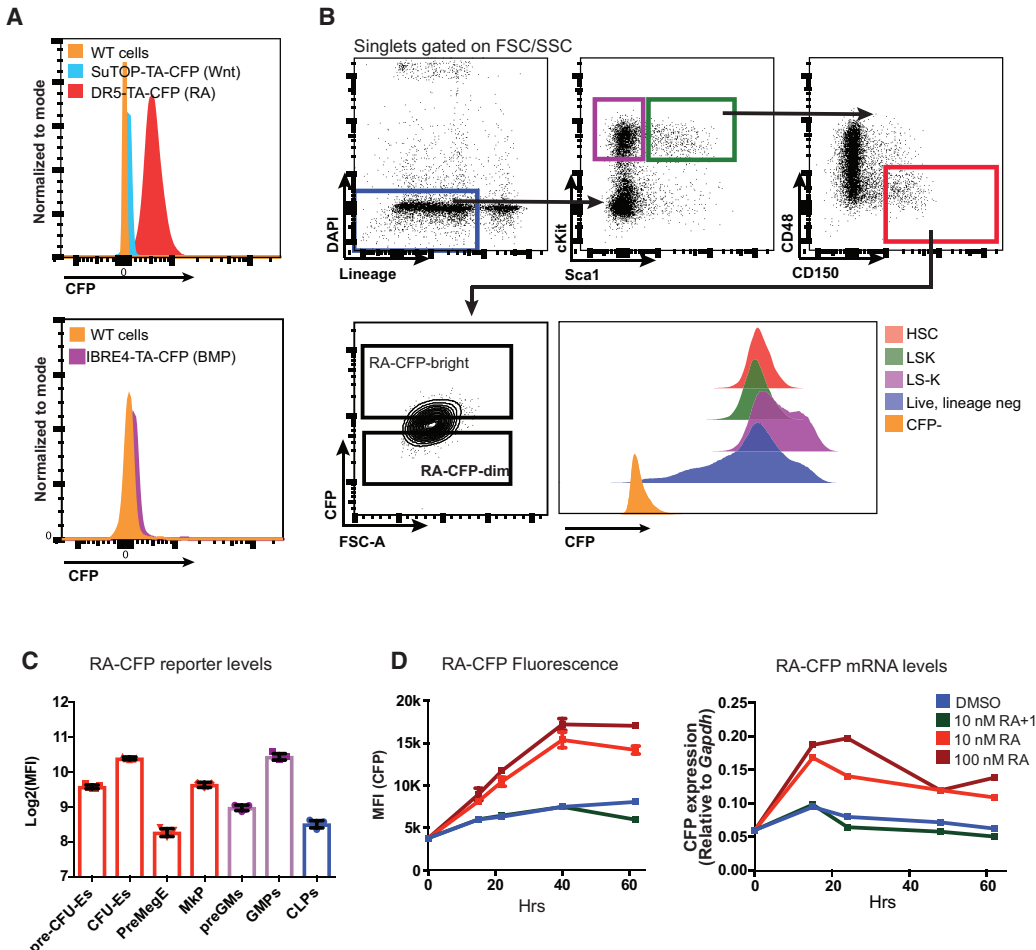


Figure 1. The DR5-TA-CFP Reporter Line Facilitates the Isolation of HSC Subpopulations

(A) CFP expression in LSK cells derived from wild-type (WT) (orange), DR5-TA-CFP (RA, red), SuTOP-TA-CFP (Wnt, blue), and IBRE4-TA-CFP (BMP, violet) reporter lines. N = 3.

(B) HSC gating strategy and RA-CFP levels in immature hematopoietic cells from the RA-CFP reporter line.

(C) RA-CFP levels in various BM progenitors from the RA-CFP reporter line. For gating strategy, see Figure S1. Abbreviations: preMegE, pre-megakaryocyte/erythroid progenitor; MkP, megakaryocytic progenitor; preGM, pre-granulocyte/macrophage; GMP, granulocyte/macrophage progenitors; CLP, common lymphoid progenitor; CFU-E, colony-forming unit erythroid; Pre-CFU-E, pre-colony-forming unit erythroid. N = 5.

(D) Response to RA stimulation in cKit⁺ cells from the RA-CFP reporter line. Cells were seeded in serum-free media with varying amounts of RA or RA + BMS493 (RA inverse agonist). Aliquots were analyzed for CFP protein (flow cytometry) or mRNA (qRT-PCR). N = 3 (three mice per replicate, three replicates). Error bars indicate SD.

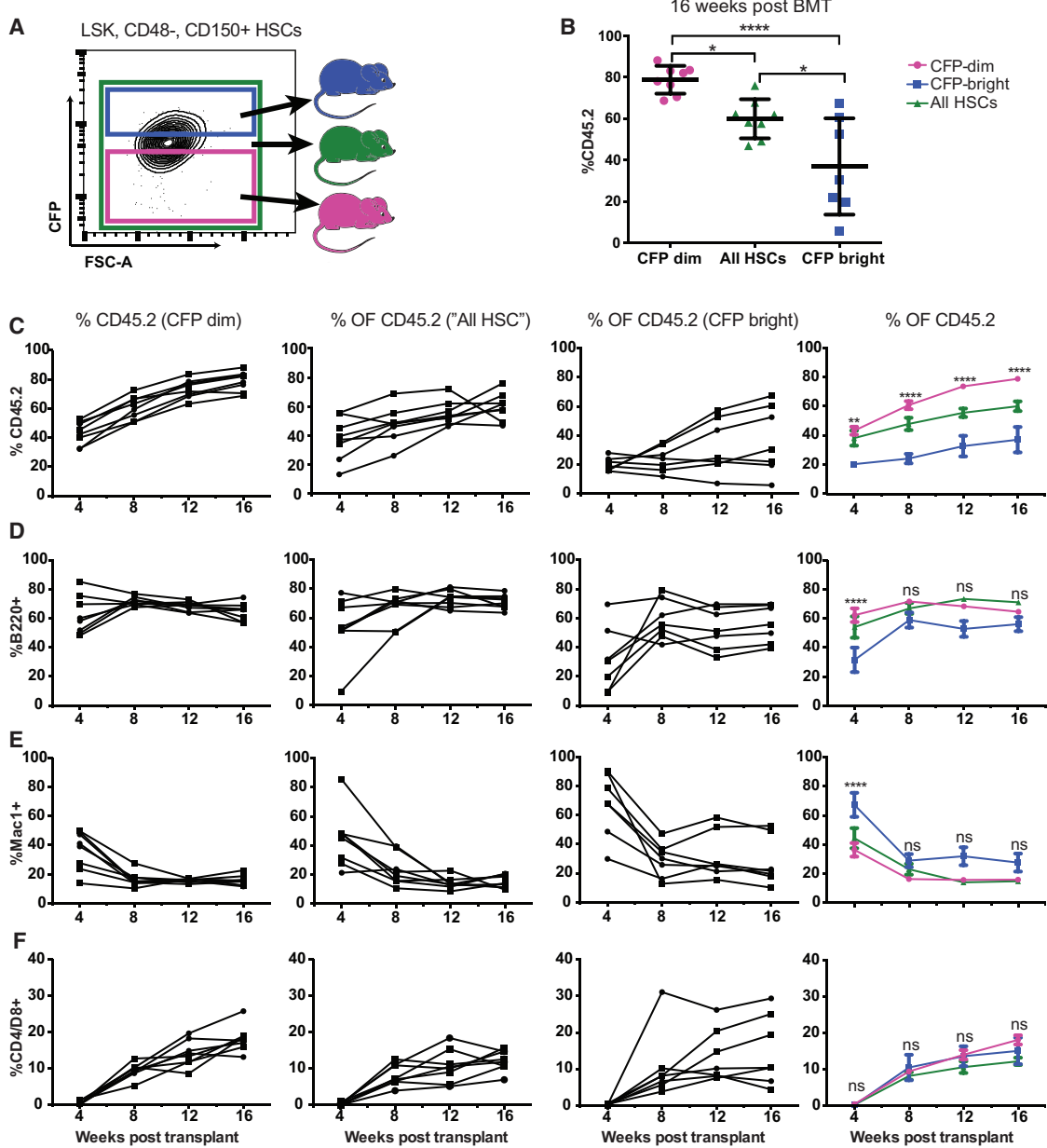
engraftment ability, with RA-CFP-dim HSCs contributing approximately twice as much as RA-CFP-bright HSCs to peripheral blood (Figures 2B and 2C). Additionally, we observed a minor difference in lineage output, with RA-CFP-dim HSCs producing significantly more B cells compared with myeloid cells and vice versa for RA-CFP-bright HSCs, although this effect leveled out over time (Figures 3D–F). The superior ability of RA-CFP-dim HSCs for hematopoietic engraftment was also observed in transplantation experiments involving HSCs derived from 14-month-old animals (Figure S2).

Taken together, low RA-CFP levels identify a subpopulation of HSCs displaying superior engraftment capability and a modest increase in B cell potential.

Transcriptome Analysis of HSCs Displaying Differential Levels of Reporter Activity

To identify transcriptional changes underlying the functional differences between the RA-CFP-dim and RA-CFP-bright HSC populations, we next performed RNA sequencing (RNA-seq) and identified a total of 318 differentially expressed genes (\log_2 fold change > 1 , $p < 0.05$; Figure 3A; Table S1).

Among these, a range of cell cycle-related genes, including *Aurka*, *Aurkab*, *Cdk1*, and *Pcna*, were markedly upregulated in the RA-CFP-bright HSCs. Consistently, gene set enrichment analysis (GSEA) identified a variety of cell cycle signatures to be enriched in this population (Figure 3B; Table S2), raising the possibility that RA-CFP reporter activity may be used to

**Figure 2. RA-CFP Levels Predict HSC Engraftment**(A) Gating strategy for CFP expression in LSK, CD48⁻, and CD150⁺ HSCs.

(B) Donor contribution in peripheral blood isolated from recipient mice transplanted with 100 HSCs (CD45.2), separated on the basis of CFP levels, and 400,000 wBM cells (CD45.1). Multiple comparisons were performed using one-way ANOVA. N = 8.

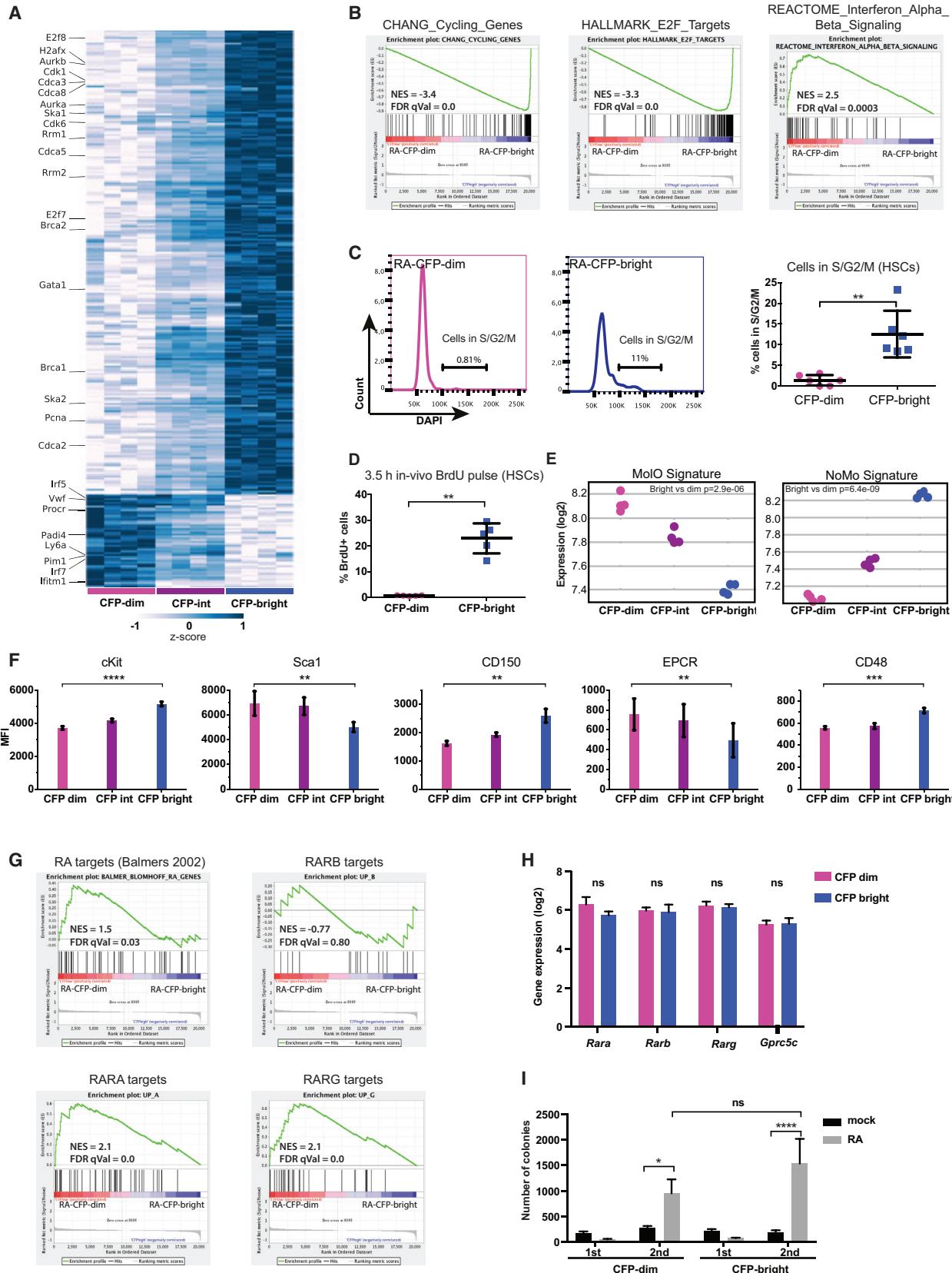
(C) As in (B) but showing the donor contribution in peripheral blood in individual and groups of mice over the time course of the experiment. Multiple comparisons were performed using two-way ANOVA. Only RA-CFP dim versus RFA-CFP bright was tested.

(D–F) Lineage contribution to peripheral blood of the three groups of donor cells: B220⁺ (D), Mac1⁺ (E), and CD4/D8⁺ (F).

Error bars indicate SD (B) or SEM (A and C–F).

distinguish between HSC populations with different proliferative properties. Consistently, cell cycle analysis demonstrated that the RA-CFP-dim HSC population was largely quiescent, whereas RA-CFP-bright HSCs displayed a larger proportion of actively cycling cells (Figures 3C and 3D). Further evidence

for their quiescent nature comes from measurements of overall protein synthesis rates demonstrating that RA-CFP-dim HSCs are significantly less metabolically active (Figure S3A). Interestingly, we also found that RA-CFP expression could be used to subdivide downstream progenitors such as short-term



(legend on next page)

HSCs (ST-HSCs) and MPP2 to MPP4 into proliferating and non-proliferating subsets (Figure S3D). We also find that cytokine-mediated cell cycle entry of HSCs *in vitro* was associated with increased RA-CFP expression, which could be further enhanced by addition of RA (Figure S3E). Collectively, these findings demonstrate that RA-CFP expression identifies proliferating subsets within the HSC and multipotent progenitor (MPP) compartments.

GSEA also identified that the expression of a number of signatures related to interferon signaling were enriched in RA-CFP-dim cells (Figure 3B; Table S2). Although *in vivo* stimulation with both interferon- α and interferon- γ has been shown to activate HSCs (Baldridge et al., 2010; Essers et al., 2009), several of the interferon-regulatory genes have been implicated in the negative regulation of cell cycle (such as *Iftm1*, *Irf5*, and *Irf6*; Bailey et al., 2008; Barnes et al., 2003; Yang et al., 2007) (Table S3). Consistent with the notion that some interferon-signaling genes may play a role in HSC quiescence, *Irgm2* and *Iftm1*, which are both upregulated in RA-CFP-dim HSCs, were previously found by mass spectrometry to be specifically expressed in HSCs compared with MPPs (Cabezas-Wallscheid et al., 2014).

In a recent study, scRNA-seq was used to identify transcriptional characteristics of HSCs isolated from a variety of protocols with the goal of capturing the essence of the HSC transcriptome (Wilson et al., 2015). Specifically, the authors identified a gene signature common to HSCs isolated from various protocols (MoLo, n = 29) and a gene signature associated with “protocol-specific” HSCs (NoMo, n = 74). Strikingly, we found that RA-CFP-dim HSCs expressed high levels of the MoLo signature genes and low levels of the NoMo signature genes (Figure 3E), further suggesting that the RA-CFP-dim phenotype is endowed with a superior HSC phenotype.

Next, we looked into the relative levels of some of the cell surface markers commonly used for HSC isolation, as these have been shown to correlate with differential HSC function. For example, decreased levels of cKit and increased levels of Sca1 identify a more quiescent HSC population with increased engraftment ability (Grinenko et al., 2014; Wilson et al., 2015). In line with the superior function of RA-CFP-dim HSCs, we found them to express decreased and increased levels of cKit and Sca1, respectively (Figure 3F). Moreover, increased expression of CD150 has previously been shown to mark a more myeloid-biased HSC population, whereas decreased levels mark a more lymphoid-biased population (Beerman et al., 2010).

Consistent with our transplantation data, we found that RA-CFP-dim HSCs express relatively low levels of CD150 (Figure 3F). Finally, and most notably, EPCR expression is markedly higher on RA-CFP-dim HSCs versus their RA-CFP-bright counterparts (Figure 3F).

Collectively, the gene expression data and cell surface marker expression are consistent with the notion that RA-CFP-dim HSCs constitute a superior HSC population within the LSK-SLAM compartment.

RA Signaling in RA-CFP-Dim and RA-CFP-Bright Populations

RA signaling has recently been implicated in the regulation of HSC dormancy (Cabezas-Wallscheid et al., 2017). To test for potential RA-regulated genes, we first assessed the expression of a previously defined RA-target gene set (Balmer and Blomhoff, 2002) and found no major differences between their expression in RA-CFP-dim and RA-CFP-bright HSCs (Figure 3G). As RA-target genes may be highly cell type dependent, we also generated RA-target gene sets on the basis of expression correlations with the three individual RA receptors across the entire ImmGEN gene expression dataset of hematopoietic cell types (Malhotra et al., 2012; Miller et al., 2012; Narayan et al., 2012). This analysis showed higher expression of specific RARA and RARG target genes in RA-CFP-dim cells, despite the similar expression levels of these receptors in our two HSC populations (Figures 3G, 3H, and S3B). Interestingly, the RA receptor target genes were only minimally overlapping, suggesting that each RAR targets highly selective genes (Figure S3C). To assess if these expression differences also translated into functional differences, we tested the response of RA-CFP-dim and RA-CFP-bright HSCs to RA for 3 days in culture, followed by serial replating in methyl cellulose. Consistent with earlier findings, RA treatment led to a marked increase in colonies following serial replating (Cabezas-Wallscheid et al., 2017) with no differences between RA-CFP-dim and RA-CFP-bright HSCs (Figure 3I).

These findings suggest that RA-CFP-dim HSCs are distinct from the recently reported GPRC5C-high HSCs (Cabezas-Wallscheid et al., 2017), and consistently we found *Gprc5c* to be expressed at similar levels in RA-CFP-dim and RA-CFP-bright HSCs (Figure 3H). Moreover, our data also demonstrate that the expression of RA-target genes does not correlate with RA-CFP expression in HSCs. Thus, this underlines the fact that

Figure 3. RA-CFP-Dim HSCs Are Associated with a Distinct Gene Expression Profile and Differential HSC Marker Expression

- (A) Heatmap indicating the 318 most deregulated genes between RA-CFP-dim and RA-CFP-bright HSCs (expression fold change 2, adjusted p value < 0.01). N = 4.
- (B) GSEA illustrating the downregulation of cell cycle genes and upregulation of interferon signaling in RA-CFP-dim HSCs.
- (C and D) Cell cycle analysis of RA-CFP-dim and RA-CFP-bright HSCs using either DAPI staining, n = 6 (C), or BrdU incorporation, n = 5 (D). Paired two-tailed t test.
- (E) Expression levels of MoLo and NoMO signature genes.
- (F) Mean fluorescence intensities (MFIs) of HSC cell surface markers as a function of CFP expression. Paired two-tailed t test for RA-CFP-dim versus RA-CFP-bright.
- (G) GSEA of RA and RAR target genes in RA-CFP-dim and RA-CFP-bright HSCs.
- (H) mRNA levels (RNA-seq) of RA receptors and *Gprc5c*.
- (I) Colony-forming potential of RA-CFP-dim and RA-CFP-bright HSCs after 3 days in liquid culture ± RA, followed by 6 days in M3434 (1st). Colonies were replated into fresh M3434 and grown for an additional 4 days (2nd). Multiple comparisons were performed by one-way ANOVA within 2nd replating groups. Error bars depict SD. N = 4.

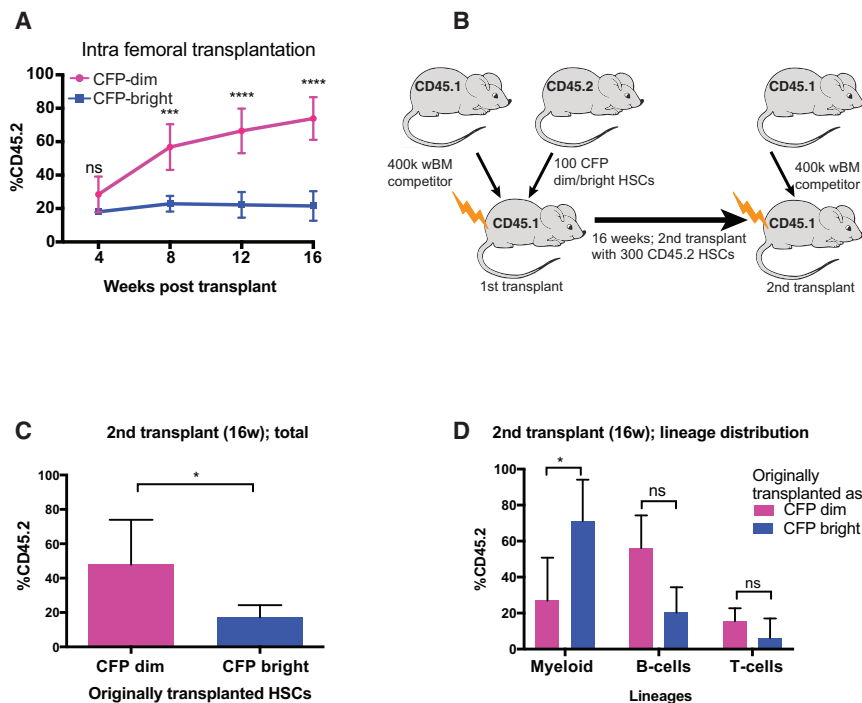


Figure 4. RA-CFP-Dim HSCs Display Higher Engraftment Levels during Serial Transplantation

(A) Donor contribution in the peripheral blood of mice subjected to intrafemoral injections with 100 RA-CFP-dim or RA-CFP-bright HSCs. Multiple comparisons were performed using two-way ANOVA. N = 6.

(B) Experimental setup for serial transplantation of mice originally transplanted with RA-CFP-dim and RA-CFP-bright HSCs.

(C) Donor contribution in the peripheral blood of secondary recipients of BM isolated from mice originally transplanted with RA-CFP-dim and RA-CFP-bright HSCs. N = 4–7.

(D) Donor contribution to different lineages in the mice from (C). Error bars indicate SD.

reporter genes are not necessarily capturing the entire complexity of signaling pathways.

RA-CFP Levels Define a Population of Label-Retaining HSCs with Increased Engraftment in Secondary Recipients

The superior engraftment levels of RA-CFP-dim HSCs in primary recipients could, in principle, reflect differences in homing efficiency between the two HSC subpopulations. To exclude this possibility, we directly injected RA-CFP-bright and RA-CFP-dim HSCs into the femoral BM cavity of irradiated recipients and compared their ability to contribute to hematopoietic regeneration. Similar to our findings using intravenous injections, RA-CFP-dim HSCs also contributed more efficiently to hematopoietic regeneration in this setting (Figure 4A).

To more rigorously test the impact of RA-CFP levels on HSC functional properties, we next performed a serial transplantation experiment (Figure 4B). Specifically, BM cells from recipient mice initially transplanted with 100 RA-CFP-bright or RA-CFP-dim HSCs, along with competitor cells, were harvested 16 weeks post-transplantation. Subsequently, 300 CD45.2⁺ HSCs (not fractionated on the basis of CFP levels) were isolated and transplanted into secondary recipients. Remarkably, mice transplanted with HSCs derived from mice originally transplanted with RA-CFP-dim HSCs continued to display increased donor contribution in secondary recipients (Figure 4C). Consistent with the results from primary recipients (Figure 2), donor contribution in these animals was skewed toward the B cell lineage at the expense of the myeloid lineage (Figure 4D).

Recently, it has been suggested that contribution of HSCs to hematopoietic output in a transplantation setting may differ

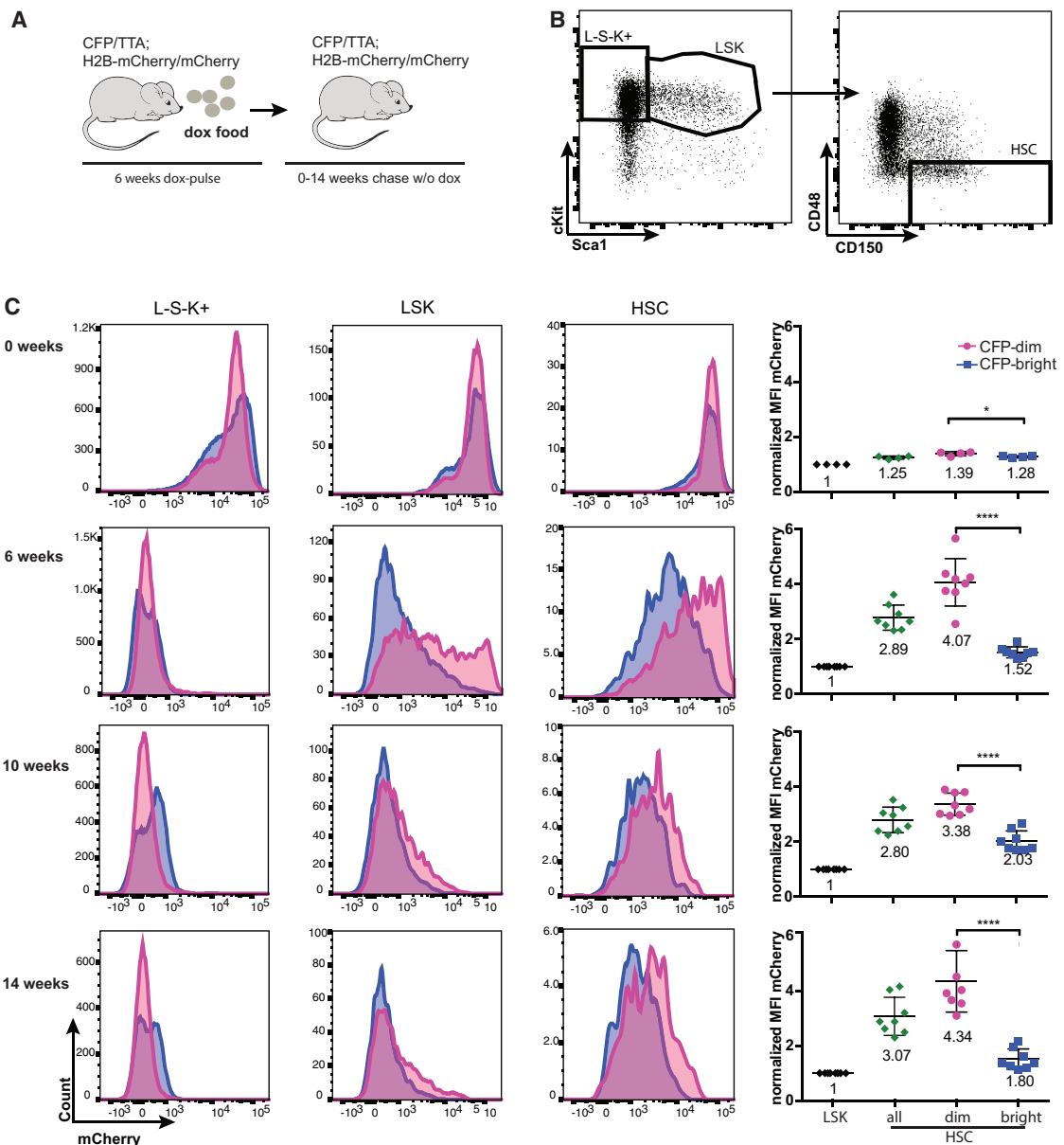
from that occurring in an unperturbed steady-state hematopoietic system (Busch et al., 2015; Sun et al., 2014). We therefore wanted to address whether RA-CFP reporter levels also affected HSC behavior in steady state, specifically whether RA-CFP-dim HSCs were enriched in the fraction of so-called label-retaining cells, which have been demonstrated to be enriched for LT-HSC activity (Wilson et al., 2008).

We therefore crossed the *Rosa26-RA-CFP* allele onto the *Rosa26-rtTA::Col1a1-tetO-H2B-mCherry* strain, which allows doxycycline (dox)-induced expression of H2B-mCherry. The resulting *Rosa26-CFP/rtTA::Col1a1-tetO-H2B-mCherry* (R26-CFP/TTA; hereafter H2B-mCherry) animals were fed for 6 weeks with dox-chow and subsequently analyzed immediately or chased for 0, 6, 10, and 14 weeks in the absence of dox (Figure 5A). Initial H2B-mCherry labeling efficiencies of HSCs, LSKs, and progenitors (L-S-K+) were high, and there were no major differences in H2B-mCherry labeling when gating on the top 10% and bottom 10% RA-CFP-expressing HSCs (i.e., RA-CFP-bright and dim, respectively) (Figures 5B and 5C; 0 weeks). In contrast, RA-CFP-dim HSCs in mice chased for 6, 10, and 14 weeks displayed consistently higher levels of H2B-mCherry, demonstrating that the RA-CFP-dim population of HSCs are enriched in label-retaining cells (Figure 5C).

Overall, these data suggest that RA-CFP-dim HSCs constitute an HSC population that is enriched in cells that support LT-HSC function, both in a steady-state and in a transplantation setting.

Whole-Genome Bisulfite Sequencing of RA-CFP-Dim and RA-CFP-Bright HSC Populations

Our data suggest that RA-CFP reporter levels can be used to distinguish subsets of HSCs with distinct functional properties. As differential epigenetic memory has previously been associated with distinct HSC functionality (Yu et al., 2016), we subjected HSCs from the RA-CFP line to genome-wide DNA methylation analysis and assembled differentially methylated regions (DMRs) into super-DMRs (Experimental Procedures).

**Figure 5. Label-Retaining HSCs Are Enriched in the RA-CFP-Dim HSC Compartment**

(A) Experimental setup.

(B) Gating strategy.

(C) Analysis of H2B-mCherry expression in progenitors (L-S-K+), LSK cells (L-S-K+), and HSCs (LSK, CD48⁻, CD150⁺) following 6 weeks of labeling in the presence of dox following a chase for the indicated times. H2B-mCherry MFI is quantified in LSKs (in order to minimize variation between experimental time-points/mice) and HSCs (unfractionated, 10% RA-CFP dim and 10% RA-CFP bright) and normalized to the levels in LSK cells of individual mice. Error bars indicate SD and significance was determined using a paired t test for RA-CFP-dim versus RA-CFP-bright. N = 4–8.

RA-CFP-dim HSCs exhibited increased overall methylation levels compared with RA-CFP-bright HSCs, consistent with the general notion that HSCs are more methylated compared with their downstream progeny (Figure S4A) (Cabezas-Wallscheid et al., 2014). Indeed, super-DMRs exhibited increased methylation mainly in RA-CFP-dim HSCs. However, this was not accompanied by systematic changes in the expression of

associated genes (Figure S4B; Table S4). Gene Ontology analysis identified developmental genes as well as bivalent genes (marked by H3K4me3 and H3K27me3 as being hypermethylated in RA-CFP-dim HSCs; Figure S4C; Table S5). Overall, this analysis suggests that RA-CFP-dim and RA-CFP-bright HSCs are associated with distinct methylation patterns but that these are not predictive of gene expression.

Single-Cell Gene Expression Reveals a Clear Correlation between RA-CFP Levels and Cell Cycle Status of HSCs

In order to expand on our initial transcriptome analysis on bulk HSC populations and to gain further insights into the potential HSC heterogeneity at the single-cell level, we performed massively parallel RNA single-cell sequencing (MARS-seq) on ~1,500 index-sorted HSCs (Jaitin et al., 2014). Clustering analysis of the 1,248 HSCs passing our quality filters revealed a total of ten transcriptional clusters. Clusters 8–10 were generally characterized by higher RA-CFP reporter expression levels and were markedly enriched for genes associated with active proliferation, such as *Pcna*, *Aurka*, and several *Mcm* genes (Figure 6A). Indeed, we found RA-CFP-dim cells to be associated mainly with the G0/G1 phase of the cell cycle on the basis of the scRNA-seq data (Figure 6B). Moreover, removal of cell cycle genes from analysis also removed most of the variance in the dataset (Figure 6C). Hence, cell cycle differences underlie the main heterogeneity within the HSC compartment. The transcriptional signatures of the remaining clusters were much weaker, although we did observe interferon pathway genes, including *Ifitm1* and *Ifitm3*, to be selectively expressed in clusters 2 and 3, which are also associated with low RA-CFP reporter expression. We also note that RA-CFP reporter expression is highly correlated with the number of unique molecular identifiers (UMIs) (i.e., reflecting the overall level of active transcription) and therefore in line with the notion that RA-CFP-bright expression marks a population of metabolically active and proliferating HSCs (Figure S4D).

Classically, hematopoietic differentiation has been linked to progressive lineage commitment, in which multipotency is gradually lost. Recent studies using single-cell analysis, however, suggest that oligopotent hematopoietic progenitors are specified toward a specific lineage, at least at a transcriptional level (Paul et al., 2015; Perié et al., 2015). Therefore, we set out to investigate the degree to which distinct lineage-specific gene expression programs were expressed in HSCs. Our initial analysis did not reveal any distinct lineage-affiliated transcriptional clusters (Figure 6A). However, we reasoned that this may be due to the low expression of such transcripts in HSCs. To more robustly detect potential lineage-affiliated gene expression programs in HSCs, we compiled four gene signatures from the literature representing HSC, myeloid, lymphoid, and erythroid/megakaryocytic gene expression programs (Experimental Procedures). We subsequently developed a two-step approach (Experimental Procedures) to cluster HSCs into a total of ten lineage-associated clusters (Figures 6D and 6E). Strikingly, all potential combinations of lineage-specific gene expression programs were detected, a finding that appears incompatible with a model in which the transcriptional priming of individual HSCs is a major determinant of hematopoietic differentiation. Importantly, we detected a similar spectrum of lineage-specific gene expression in previously published HSC RNA-seq datasets (Figure S4E).

We next performed a network analysis of our scRNA-seq HSC data. In line with our initial clustering analysis, clusters 8–10 and RA-CFP-bright cells located to the same part of the network, further demonstrating the close association between prolifera-

tion and RA-CFP reporter expression (Figures 6F and 6G). In contrast, cells expressing myeloid, lymphoid, or erythroid/megakaryocytic gene signatures were scattered over the entire network, further arguing against the notion that specific HSC subpopulations are transcriptionally primed toward specific hematopoietic lineages (Figures S4F–S4H).

In a final attempt to explore the potential transcriptional heterogeneity within the HSC compartment, we generated diffusion pseudotime maps of the HSC scRNA-seq data, which revealed the presence of two distinct clusters (Figure 7A). Pathway analysis suggested that the transition from early to late pseudotime was associated with an increase in the term Translation_Factors, indicating that translation is more active in the late cluster (Figure 7B; Table S6). This is also supported by studies of individual genes demonstrating that two members of the TRiC/CCT chaperone complex, which is involved in protein folding (Broadley and Hartl, 2009) and likely required in cells with high protein synthesis activity, are markedly upregulated in the late cluster (Figure 7C; Table S7). Although the late cluster displayed a slightly elevated cell cycle score, this did not correlate with the Translation_Factors term, suggesting that these features are mutually independent and that early and late cluster cells replicate to the same extent (Figures 7B and 7D).

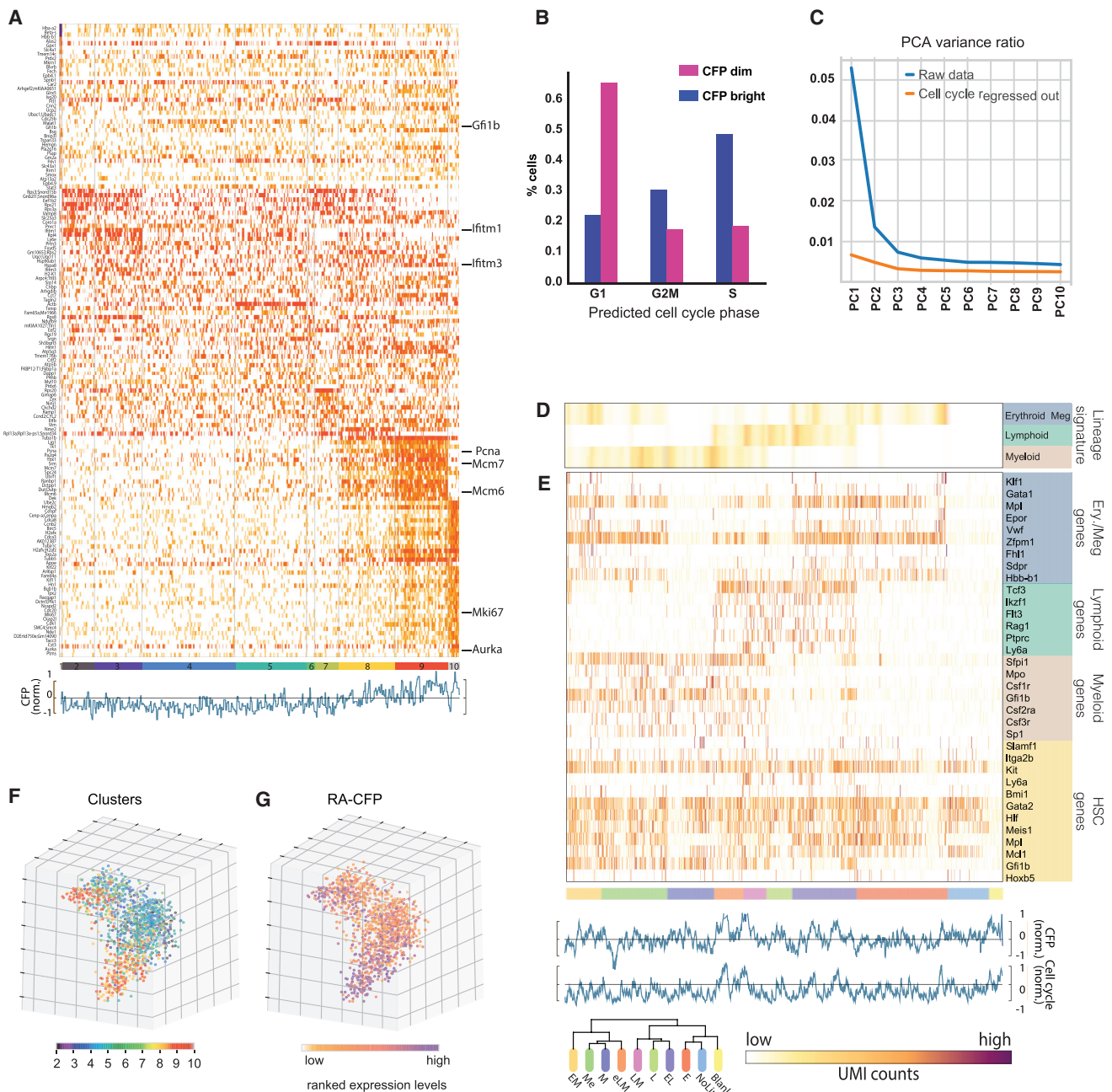
Taken together, our scRNA-seq data demonstrate that the transcriptomes of individual HSCs are very homogeneous and that the main driver of HSC heterogeneity is differences in cell cycle status.

DISCUSSION

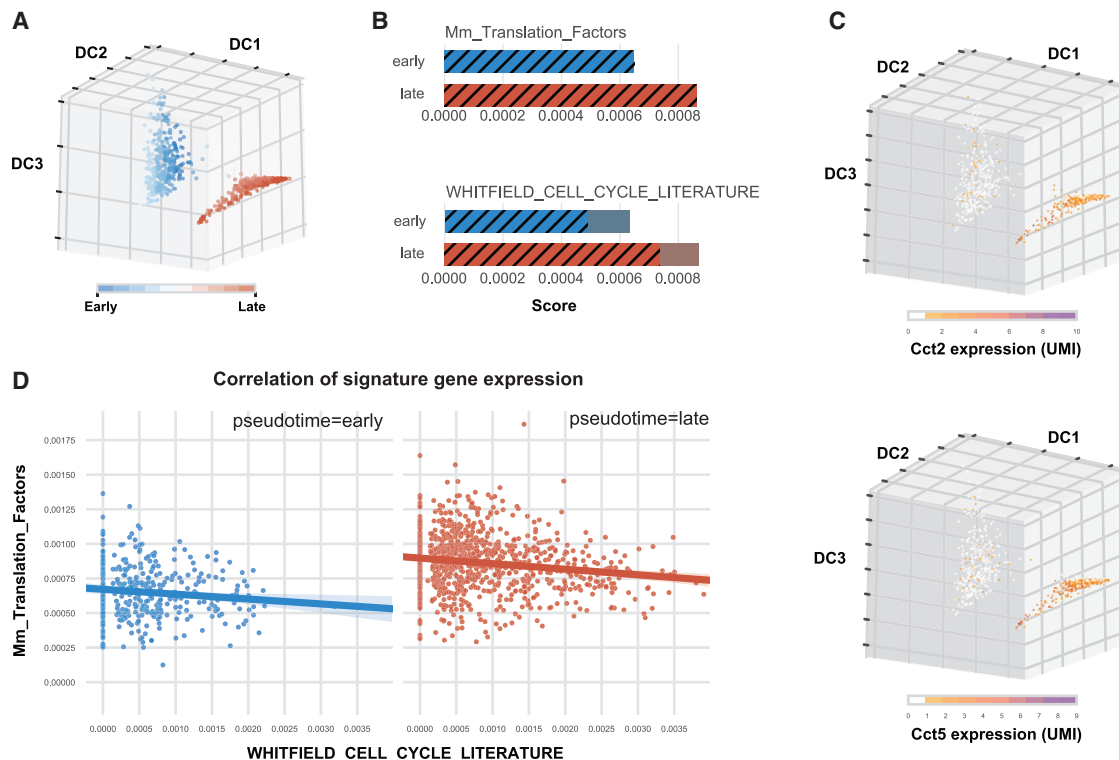
Even though current HSC isolation strategies result in high levels of HSC purity, as measured by engraftment ability in single-cell transplantation studies, HSC populations remain functionally heterogeneous in terms of lineage output and long-term engraftment capabilities. In this study, we investigated whether we could use murine reporter models for cellular signaling pathways in order to further resolve heterogeneity within the HSC compartment.

The RA-CFP Reporter Line Facilitates the Isolation of Superior HSCs

By using a RA-CFP reporter line, which displays a tight and intermediate level of CFP expression in HSCs, we were able to subfractionate the LSK SLAM HSC compartment into functionally distinct HSCs. Specifically, RA-CFP-dim HSCs were largely quiescent and displayed significantly enhanced abilities of hematopoietic reconstitution. In contrast, RA-CFP-bright cells engrafted relatively poorly and were highly proliferative. Strikingly, the superior phenotype of the RA-CFP-dim HSCs was maintained in secondary recipients, which suggests a limited transition between the RA-CFP-dim and RA-CFP-bright HSCs over time and throughout challenges. This is supported not only by the DNA methylation differences between these populations but also by the observation that the RA-CFP-dim population is enriched in label-retaining LT-HSCs. Further characterization of the RA-CFP-dim HSCs demonstrated that these cells were associated with high Sca1, high EPCR, relatively lower CD150 expression, and low cKit expression, thereby re-capitulating a previously reported

**Figure 6. ScRNA-Seq Analysis of RA-CFP HSCs**

- (A) Heatmap indicating the expression levels (UMIs) of the 149 most variable genes from the HSC ScRNA-seq data. The corresponding RA-CFP values (normalized) are shown below.
- (B) Individual RA-CFP-dim and RA-CFP-bright cells were assigned to the G0/G1, G2M, and S phases of the cell cycle.
- (C) The contribution of the individual principal components to the variance of the data before and after removal of cell cycle genes.
- (D) Lineage signature scores for single cells.
- (E) Heatmap showing the expression of individual lineage signature genes. The corresponding RA-CFP and cell cycle score values are depicted below. The hierarchical organization of the single-cell lineage clusters is also shown.
- (F) SPRING-based three-dimensional (3D) network representation of the scRNA-seq data. Colors of each individual cells depict the cluster numbers from (A).
- (G) Same as (D) but depicting RA-CFP expression levels (ranked for visualization purposes) in individual HSCs.

**Figure 7. Pseudotime Analysis of RA-CFP HSCs**

- (A) Diffusion map of individual cells color-coded as a function of pseudotime.
- (B) Gene expression signature scores for early (pseudotime < 0.5) and late (pseudotime > 0.5) clusters of individual HSCs. The height represents the mean expression score of the signature, whereas the height of the inner bar depicts the frequency of cells with a signature different from zero.
- (C) Gene expression of CCT factors in individual HSC superimposed on the diffusion map.
- (D) Correlation of signature gene expression in individual HSCs. The early and late pseudotime clusters are depicted separately.

marker code for high-end HSCs (Wilson et al., 2015). Finally, the transcriptome of RA-CFP-dim HSCs correlated tightly with the MolO gene expression signature (i.e., genes associated with functional HSCs across different cell surface marker panels) (Wilson et al., 2015). Collectively, these findings demonstrate that RA-CFP-dim HSCs share multiple properties of high-end HSCs and that the RA-CFP-reporter line constitutes a simple, yet efficient, tool for their prospective isolation.

RA Signaling in the HSC Compartment

In contrast to what has been reported in the human system, RA signaling in mice has been associated with increased HSC self-renewal, and knockout experiments point toward the RARG isoform as the main RA receptor (Cabezas-Wallscheid et al., 2017; Purton et al., 2006). The RA reporter model used in the present study reports on the activity of a DR5 RARE, originally derived from the *Rarb* promoter, which can be bound by both RXR/RARA and RXR/RARG heterodimers (de Thé et al., 1990; Delacroix et al., 2010). Consequently, the reporter does not allow a precise distinction between the actions of the different RARs.

RA signaling leads to highly tissue specific gene expression changes. In order to correlate the behavior of the RA-CFP reporter with gene expression, we generated RAR-specific target gene lists using a correlative approach. Through this approach,

we observed higher expression of RARA and RARG target genes in RA-CFP-dim HSCs compared with their RA-CFP-bright counterparts, suggesting that RA signaling is increased in the superior RA-CFP-dim compartment *in vivo*. These findings are consistent with previous work demonstrating RA signaling in dormant GPRC5⁺ HSCs (Cabezas-Wallscheid et al., 2017). However, the RA-CFP-dim and GPRC5⁺ HSCs are clearly not identical, as *Gprc5c* expression is not increased in RA-CFP-dim HSCs. Moreover, RA markedly promotes the serial re-plating abilities of both RA-CFP-dim and RA-CFP-bright HSCs demonstrating that both populations can respond efficiently to RA. These data are consistent with a model in which RA-CFP-dim and RA-CFP-bright HSCs are located in different anatomical positions within the BM, where they experience different levels of RA signaling stimuli.

Collectively, we can conclude that RA-CFP levels in HSCs correlate inversely with the expression of three distinct RA-target gene sets. RA-CFP-dim HSCs appear to have the highest levels of RA signaling pathway activation *in vivo*. Although this finding does not detract from the fact that the RA-CFP reporter line allows sub-fractionation of the HSC compartment, it obviously raises concerns regarding the use of reporter mice reporting on single, multimerized transcription factor binding sites as indicators of pathway activity.

RA-CFP-Dim and RA-CFP-Bright HSCs Display Distinct Gene Expression Profiles

In line with the marked functional difference in their proliferative behavior, RA-CFP-dim HSCs were associated with a marked reduction in the expression of cell cycle-related genes. It has previously been reported that the proliferative status of hematopoietic stem and progenitor cells (HSPCs) and HSCs is important for their engraftment ability and that the proliferating subsets of HSPCs and HSCs display a diminished reconstitution potential of irradiated hosts (Bowie et al., 2006; Nygren et al., 2006). Some of these studies have suggested that this is due to the cell cycle-specific expression of receptors important for homing of HSCs. However, RA-CFP-dim and RA-CFP-bright HSCs do not differ in their expression of genes encoding important receptors for HSC homing, including *Cxcr4*, *Cd44*, *LFA-1*, or *Vla4* (data not shown), arguing against cell cycle-driven differences in homing as the underlying mechanism. In line with this, intrafemoral injection of HSCs results in similar functional differences between RA-CFP-dim and -bright HSCs. Moreover, the 12%–20% of actively replicating RA-CFP-bright HSCs are unlikely to account for the 2-fold reduction in hematopoietic engraftment observed in this population. Instead, we favor a model in which the activated cell cycle status of the RA-CFP-bright HSCs renders them more likely to differentiate and consequently contribute less to hematopoietic reconstitution than their RA-CFP-dim counterparts.

Finally, we also noted a prominent enrichment of several gene expression signatures related to interferon signaling in RA-CFP-dim HSCs. Although interferon- α and interferon- γ are activators of HSCs *in vivo* and are known to promote cell cycle entry (Baldridge et al., 2010; Essers et al., 2009), several of the interferon signature genes have previously been reported to be enriched specifically in HSCs (Cabezas-Wallscheid et al., 2014; Wilson et al., 2015). Moreover, several of the interferon signature genes have been shown to be important for promoting growth arrest in other contexts (Table S3). Consequently, these findings suggest both that interferon signaling is associated with the exit of HSCs from quiescence and that a certain baseline level is required for HSC maintenance. This in turn suggests that interferon signaling, or at least the expression of certain interferon signaling signature genes, must be tightly controlled in HSCs in order to prevent HSC exhaustion.

Cell Cycle Progression Is the Main Source of Transcriptional Heterogeneity within the HSC Compartment

The inability to prospectively isolate an HSC population with uniform behavior in assays for HSC function has led to the widespread notion that the HSC compartment is heterogeneous. This view is supported by single-cell transplantation experiments demonstrating lineage-biased behavior of HSCs as exemplified by the myeloid-biased α -HSCs, platelet-biased *Vwf⁺*-HSCs, and others (Dykstra et al., 2007; Sanjuan-Pla et al., 2013). However, in each case only an increase in the propensity to give rise to a certain lineage(s) is observed, raising the possibility that the propensity for an HSC to differentiate toward a certain lineage is not hard wired but may instead represent stochastic changes in gene expression. To characterize HSC heterogeneity at a

higher resolution than previously reported, we transcriptionally profiled >1,200 HSCs using MARS-seq and found cell cycle activity to be responsible for the main transcriptional variance within the HSC compartment. Moreover, as the cell cycle-active clusters are associated with high levels of RA-CFP at the single-cell level, this finding not only supports conclusions from previous scRNA-seq studies using much lower cell numbers but also couples cell cycle status, inferred by RA-CFP levels, to HSC performance (Kowalczyk et al., 2015; Tsang et al., 2015).

Apart from the cell cycle-active clusters, we observed a very limited degree of transcriptional heterogeneity within the HSC compartment. However, when focusing on lineage-affiliated genes, we observed a significant degree of transcriptional heterogeneity driven by the low expression of these genes. Strikingly, we identified transcriptional clusters expressing myeloid, lymphoid, or erythroid/megakaryocytic programs as well as combinations thereof. However, as these clusters displayed only limited correlation with RA-CFP levels and consequently HSC performance, the most parsimonious explanation is that they originate from stochastic low-level expression of lineage programs, perhaps driven by low-abundance expression of lineage-specific regulators. A similar model has previously been forwarded on the basis of experiments in a multipotent cell line (Hu et al., 1997), but in this study we address this phenomenon in the context of >1,200 highly purified HSCs. Finally, as a natural extension of this model it is tempting to hypothesize that the stochastic sampling of lineage-affiliated transcriptional programs is what endows individual HSCs with an increased probability to adopt a certain fate.

In summary, we have demonstrated the utility of the RA-CFP reporter line for sub-fractionation of the HSC compartment. RA-CFP-dim HSCs are largely quiescent, express higher levels of interferon-signaling genes, and are associated with superior engraftment abilities. Single-cell transcriptome analysis demonstrates a stochastic low-level expression of lineage-affiliated genes, which may underlie previously reported lineage biases of individual HSCs. However, the main functional variance within the HSC compartment is associated with cell cycle activity. This variance can be resolved in the RA-CFP reporter line, which we predict will be of wide interest to the HSC community.

EXPERIMENTAL PROCEDURES

Mice and Mouse Procedures

Mice were housed at the Department for Experimental Medicine at the University of Copenhagen according to institutional guidelines. All animal work was approved by the Danish Animal Ethical Committee and by the review board at the Faculty of Health Sciences, University of Copenhagen.

The generation of the -60/DR5-TA-RA-CFP, SuTOP-TA-CFP (Wnt signaling), and IBRE4-TA-CFP (BMP signaling) mouse strains was described previously (Serup et al., 2012).

For transplantation assays, young females (10–14 weeks, -60/DR5-TA-RA-CFP Ly-5.2/CD45.2) were used as donors, unless otherwise stated. One hundred donor cells were transplanted into young (10–14 weeks) congenic (Ly-5.1/CD45.1) recipients through tail vein injection. Recipients were lethally irradiated (900 cGy) 24 hr prior to transplantation. As support 400,000 CD45.1 wBM cells were transplanted alongside. Post-irradiation mice were supplemented with ciprofloxacin in the drinking water (100 mg/L; Actavis or Sigma) for 4 weeks. A blood sample was drawn from the facial vein every 4 weeks for analysis.

For intrafemoral transplants, lethally irradiated recipients (under isoflurane anesthesia) received 100 RA-CFP-dim or RA-CFP-high HSCs in a volume of 20 µL PBS in the right femur. In addition, the recipients were transplanted with 325,000 wBM cells (intravenously [i.v.]) 5 hr prior to the procedure and received three 0.1 mg doses of Rimadyl SC for 3 days post-transplantation.

For label-retaining experiments, we intercrossed the *Rosa26-RA-CFP* allele and *Rosa26-rtTA::Col1a1-tetO-H2B-mCherry* (Jax mice stock number 014602) in order to generate *Rosa26-CFP/rtTA::Col1a1-tetO-H2B-mCherry* experimental animals (Beard et al., 2006; Egli et al., 2007). Expression of H2B-mCherry was induced by keeping 10- to 14-week-old females on dox-containing food pellets (2,000 mg/kg; Ssniff Spezialdiäten) for 6 weeks, followed by a chase for 0–14 weeks.

Flow Cytometry

Tibia, femur, and iliac bones were harvested from experimental animals and crushed in PBS + 3% fetal calf serum (FCS). For the sorting of HSPC populations, BM cells were cKit enriched prior to antibody staining. Briefly, cells were resuspended in 200 µL PBS + 3% FCS and incubated with 7 µL CD117 magnetic microbeads for 30 min and purified on magnetic separation columns following the manufacturer's protocol (Miltenyi Biotec). Prior to antibody staining of peripheral blood, 30 µL of blood was lysed twice to remove red blood cells using Pharmlyse (BD) according to the manufacturer's protocol. Antibodies are listed in the *Supplemental Information*.

All flow cytometry involving analysis and sort of CFP was carried out on a FACS AriaIII (BD) equipped with a custom 445 nm deep-blue laser. To record the intensity of surface markers used for sorting of single cells for RNA-seq, the FACS DIVA “index sorting” function was activated. Blood samples were analyzed on either an Accuri C6 (BD) or a FACSCanto (BD). Subsequent analysis was performed using FlowJo (Treestar).

In Vitro Assays

In order to assess RA-reporter response *in vitro*, cKit⁺ cells were sorted by FACS and grown in StemSpan serum-free media (StemCell Technologies) supplemented with 1% penicillin-streptomycin (PenStrep), 50 ng/mL murine stem cell factor (PeproTech), and 50 ng/mL human thrombopoietin (PeproTech). RA (ATRA) and BMS493 (both from Sigma-Aldrich) were dissolved in DMSO.

To assess the serial replating potential of RA-CFP-dim and RA-CFP-bright HSCs, we plated 400 HSCs in 96 individual wells and cultured them in 100 µL StemPro-34 SFM (Life Technologies), supplemented with murine SCF 50 ng/mL, murine TPO 25 ng/mL, 30 ng/mL human Flt3-ligand (all PeproTech), 100 U/mL PenStrep, and 2 mM L-glutamine in the presence of 5 µM RA/vehicle (DMSO). Cells were cultured for 72 hr and the contents of 96 individual wells were transferred into M3434 semisolid medium (StemCell Technologies) supplemented with 100 U/mL PenStrep. Colonies were counted after 6 days, and 30,000 cells were transferred into fresh M3434 semisolid medium. Following 4 additional days of culturing, colonies were counted.

RNA-Sequencing Analysis

ScRNA-Seq

Single HSCs were index-sorted into cold 384-well capture plates containing 2 µL of cell lysis solution and barcoded poly(T) RT primers for scRNA-seq. cDNA from barcoded single cells was pooled using an automated pipeline (Jaitin et al., 2014). The pooled sample was amplified, and the resulting RNA was fragmented and converted into a sequencing-ready library by tagging the samples with pool barcodes and Illumina sequences during subsequent steps (ligation, RT, and PCR) (Jaitin et al., 2014). Libraries were sequenced on a NextSeq500, and data were deposited in the GEO repository under accession number GEO: GSE108155.

Each pool of cells was tested for library quality, and concentration was assessed as described earlier (Jaitin et al., 2014). Cells not meeting the quality standards were removed from the subsequent analyses; 1,248 of 1,520 sorted cells met the quality thresholds.

Purification of RNA for Population-Based RNA-Seq

HSCs were separated into three groups depending on their CFP levels (~20% brightest, dimmest, and an intermediate group) and 400–1,000 cells were sorted into 50 µL of LiDS lysis/binding buffer (Life Technologies). mRNA was

captured with 12 µL of Dynabeads oligo(dT) (Life Technologies), washed, and eluted with 10 µL of 10 mM Tris-HCl buffer (pH 7.5). To produce gene expression libraries, a derivation of the protocol used for generating the single-cell expression libraries was used (Jaitin et al., 2014). Libraries were sequenced on a NextSeq500, and data were deposited in the GEO repository under accession number GEO: GSE108155.

Statistical Analysis

Student's t test and one- and two-way ANOVA were used for statistical tests (*p < 0.05, **p < 0.01, ***p < 0.001, and ****p < 0.0001).

Bioinformatics

Details regarding bioinformatic data processing are given in the *Supplemental Information*.

DATA AND SOFTWARE AVAILABILITY

The accession number for the library data reported in this paper is GEO: GSE108155.

SUPPLEMENTAL INFORMATION

Supplemental Information includes four figures and seven tables and can be found with this article online at <https://doi.org/10.1016/j.celrep.2018.06.057>.

ACKNOWLEDGMENTS

This study was supported through a center grant from the Novo Nordisk Foundation (Novo Nordisk Foundation Center for Stem Cell Biology, DanStem; grant NNF17CC0027852). We thank Anna Fossum and Gelo Dela Cruz for their help with cell sorting and members of the Porse lab for discussions.

AUTHOR CONTRIBUTIONS

F.K.B.L., T.L.J., A.S.W., F.P., M.S.H., and M.R. performed experiments. F.K.B.L., T.L.J., N.R., D.A., A.G., S.P., M.S.H., I.A., and B.T.P. analyzed data. F.K.B.L., T.L.J., M.S.H., I.A., M.R., and B.T.P. designed experiments. P.S. contributed reporter mice. F.K.B.L., T.L.J., and B.T.P. drafted the manuscript. All authors proofread and approved the final version of the manuscript.

DECLARATION OF INTEREST

The authors declare no competing interests.

Received: December 18, 2017

Revised: May 25, 2018

Accepted: June 14, 2018

Published: July 17, 2018

REFERENCES

- Bailey, C.M., Abbott, D.E., Margaryan, N.V., Khalkhali-Ellis, Z., and Hendrix, M.J. (2008). Interferon regulatory factor 6 promotes cell cycle arrest and is regulated by the proteasome in a cell cycle-dependent manner. *Mol. Cell. Biol.* 28, 2235–2243.
- Baldridge, M.T., King, K.Y., Boles, N.C., Weksberg, D.C., and Goodell, M.A. (2010). Quiescent hematopoietic stem cells are activated by IFN-gamma in response to chronic infection. *Nature* 465, 793–797.
- Balmer, J.E., and Blomhoff, R. (2002). Gene expression regulation by retinoic acid. *J. Lipid Res.* 43, 1773–1808.
- Barnes, B.J., Kellum, M.J., Pinder, K.E., Frisachio, J.A., and Pitha, P.M. (2003). Interferon regulatory factor 5, a novel mediator of cell cycle arrest and cell death. *Cancer Res.* 63, 6424–6431.
- Beard, C., Hochedlinger, K., Plath, K., Wutz, A., and Jaenisch, R. (2006). Efficient method to generate single-copy transgenic mice by site-specific integration in embryonic stem cells. *Genesis* 44, 23–28.

- Beerman, I., Bhattacharya, D., Zandi, S., Sigvardsson, M., Weissman, I.L., Bryder, D., and Rossi, D.J. (2010). Functionally distinct hematopoietic stem cells modulate hematopoietic lineage potential during aging by a mechanism of clonal expansion. *Proc. Natl. Acad. Sci. U S A* 107, 5465–5470.
- Bernitz, J.M., Kim, H.S., MacArthur, B., Sieburg, H., and Moore, K. (2016). Hematopoietic Stem Cells Count and Remember Self-Renewal Divisions. *Cell* 167, 1296–1309.e10.
- Bowie, M.B., McKnight, K.D., Kent, D.G., McCaffrey, L., Hoodless, P.A., and Eaves, C.J. (2006). Hematopoietic stem cells proliferate until after birth and show a reversible phase-specific engraftment defect. *J. Clin. Invest.* 116, 2808–2816.
- Broadley, S.A., and Hartl, F.U. (2009). The role of molecular chaperones in human misfolding diseases. *FEBS Lett.* 583, 2647–2653.
- Busch, K., Klapproth, K., Barile, M., Flossdorf, M., Holland-Letz, T., Schlenner, S.M., Reth, M., Höfer, T., and Rodewald, H.R. (2015). Fundamental properties of unperturbed haematopoiesis from stem cells in vivo. *Nature* 518, 542–546.
- Cabezas-Wallscheid, N., Klimmeck, D., Hansson, J., Lipka, D.B., Reyes, A., Wang, Q., Weichenhan, D., Lier, A., von Paleske, L., Renders, S., et al. (2014). Identification of regulatory networks in HSCs and their immediate progeny via integrated proteome, transcriptome, and DNA methylome analysis. *Cell Stem Cell* 15, 507–522.
- Cabezas-Wallscheid, N., Buettner, F., Sommerkamp, P., Klimmeck, D., Ladel, L., Thalheimer, F.B., Pastor-Flores, D., Roma, L.P., Renders, S., Zeisberger, P., et al. (2017). Vitamin A-retinoic acid signaling regulates hematopoietic stem cell dormancy. *Cell* 169, 807–823.e19.
- Chute, J.P., Muramoto, G.G., Whitesides, J., Colvin, M., Safi, R., Chao, N.J., and McDonnell, D.P. (2006). Inhibition of aldehyde dehydrogenase and retinoid signaling induces the expansion of human hematopoietic stem cells. *Proc. Natl. Acad. Sci. U S A* 103, 11707–11712.
- Cunningham, T.J., and Duester, G. (2015). Mechanisms of retinoic acid signalling and its roles in organ and limb development. *Nat. Rev. Mol. Cell Biol.* 16, 110–123.
- de Thé, H., Vivanco-Ruiz, M.M., Tiollais, P., Stunnenberg, H., and Dejean, A. (1990). Identification of a retinoic acid responsive element in the retinoic acid receptor beta gene. *Nature* 343, 177–180.
- Delacroix, L., Moutier, E., Altobelli, G., Legras, S., Poch, O., Choukallah, M.A., Bertin, I., Jost, B., and Davidson, I. (2010). Cell-specific interaction of retinoic acid receptors with target genes in mouse embryonic fibroblasts and embryonic stem cells. *Mol. Cell. Biol.* 30, 231–244.
- Dewamitta, S.R., Joseph, C., Purton, L.E., and Walkley, C.R. (2014). Erythroid-extrinsic regulation of normal erythropoiesis by retinoic acid receptors. *Br. J. Haematol.* 164, 280–285.
- Dykstra, B., Kent, D., Bowie, M., McCaffrey, L., Hamilton, M., Lyons, K., Lee, S.J., Brinkman, R., and Eaves, C. (2007). Long-term propagation of distinct hematopoietic differentiation programs in vivo. *Cell Stem Cell* 1, 218–229.
- Egli, D., Rosains, J., Birkhoff, G., and Eggan, K. (2007). Developmental reprogramming after chromosome transfer into mitotic mouse zygotes. *Nature* 447, 679–685.
- Essers, M.A., Offner, S., Blanco-Bose, W.E., Waibler, Z., Kalinke, U., Duchosal, M.A., and Trumpp, A. (2009). IFN α activates dormant hematopoietic stem cells in vivo. *Nature* 458, 904–908.
- Grinenko, T., Arndt, K., Portz, M., Mende, N., Günther, M., Cosgun, K.N., Alexopoulos, D., Lakshmanaperumal, N., Henry, I., Dahl, A., and Waskow, C. (2014). Clonal expansion capacity defines two consecutive developmental stages of long-term hematopoietic stem cells. *J. Exp. Med.* 211, 209–215.
- Hu, M., Krause, D., Greaves, M., Sharkis, S., Dexter, M., Heyworth, C., and Enver, T. (1997). Multilineage gene expression precedes commitment in the hematopoietic system. *Genes Dev.* 11, 774–785.
- Jaitin, D.A., Kenigsberg, E., Keren-Shaul, H., Elefant, N., Paul, F., Zaretsky, I., Mildner, A., Cohen, N., Jung, S., Tanay, A., and Amit, I. (2014). Massively parallel single-cell RNA-seq for marker-free decomposition of tissues into cell types. *Science* 343, 776–779.
- Kowalczyk, M.S., Tirosh, I., Heckl, D., Rao, T.N., Dixit, A., Haas, B.J., Schneider, R.K., Wagers, A.J., Ebert, B.L., and Regev, A. (2015). Single-cell RNA-seq reveals changes in cell cycle and differentiation programs upon aging of hematopoietic stem cells. *Genome Res.* 25, 1860–1872.
- Malhotra, D., Fletcher, A.L., Astarita, J., Lukacs-Kornek, V., Tayalia, P., Gonzalez, S.F., Elpek, K.G., Chang, S.K., Knoblich, K., Hemler, M.E., et al.; Immunological Genome Project Consortium (2012). Transcriptional profiling of stroma from inflamed and resting lymph nodes defines immunological hallmarks. *Nat. Immunol.* 13, 499–510.
- Miller, J.C., Brown, B.D., Shay, T., Gautier, E.L., Jojic, V., Cohain, A., Pandey, G., Leboeuf, M., Elpek, K.G., Hefti, J., et al.; Immunological Genome Consortium (2012). Deciphering the transcriptional network of the dendritic cell lineage. *Nat. Immunol.* 13, 888–899.
- Morrison, S.J., and Scadden, D.T. (2014). The bone marrow niche for hematopoietic stem cells. *Nature* 505, 327–334.
- Narayan, K., Sylvia, K.E., Malhotra, N., Yin, C.C., Martens, G., Vallerskog, T., Kornfeld, H., Xiong, N., Cohen, N.R., Brenner, M.B., et al.; Immunological Genome Project Consortium (2012). Intrathymic programming of effector fates in three molecularly distinct $\gamma\delta$ T cell subtypes. *Nat. Immunol.* 13, 511–518.
- Nygren, J.M., Bryder, D., and Jacobsen, S.E. (2006). Prolonged cell cycle transit is a defining and developmentally conserved hemopoietic stem cell property. *J. Immunol.* 177, 201–208.
- Passegué, E., Wagers, A.J., Giurato, S., Anderson, W.C., and Weissman, I.L. (2005). Global analysis of proliferation and cell cycle gene expression in the regulation of hematopoietic stem and progenitor cell fates. *J. Exp. Med.* 202, 1599–1611.
- Paul, F., Arkin, Y., Giladi, A., Jaitin, D.A., Kenigsberg, E., Keren-Shaul, H., Winter, D., Lara-Astiaso, D., Gury, M., Weiner, A., et al. (2015). Transcriptional heterogeneity and lineage commitment in myeloid progenitors. *Cell* 163, 1663–1677.
- Perié, L., Duffy, K.R., Kok, L., de Boer, R.J., and Schumacher, T.N. (2015). The branching point in erythro-myeloid differentiation. *Cell* 163, 1655–1662.
- Purton, L.E., Bernstein, I.D., and Collins, S.J. (1999). All-trans retinoic acid delays the differentiation of primitive hematopoietic precursors (lin⁻kit^{+/-}Scal⁺) while enhancing the terminal maturation of committed granulocyte/monocyte progenitors. *Blood* 94, 483–495.
- Purton, L.E., Bernstein, I.D., Collins, S.J., Purton, L.E., Bernstein, I.D., and Collins, S.J. (2000). All-trans retinoic acid enhances the long-term repopulating activity of cultured hematopoietic stem cells. *Blood* 95, 470–477.
- Purton, L.E., Dworkin, S., Olsen, G.H., Walkley, C.R., Fabb, S.A., Collins, S.J., and Champon, P. (2006). RAR γ is critical for maintaining a balance between hematopoietic stem cell self-renewal and differentiation. *J. Exp. Med.* 203, 1283–1293.
- Qiu, J., Papatsenko, D., Niu, X., Schaniel, C., and Moore, K. (2014). Divisional history and hematopoietic stem cell function during homeostasis. *Stem Cell Reports* 2, 473–490.
- Sanjuan-Pla, A., Macaulay, I.C., Jensen, C.T., Woll, P.S., Luis, T.C., Mead, A., Moore, S., Carella, C., Matsuoka, S., Bouriez Jones, T., et al. (2013). Platelet-biased stem cells reside at the apex of the hematopoietic stem-cell hierarchy. *Nature* 502, 232–236.
- Sawai, C.M., Babovic, S., Upadhyaya, S., Knapp, D.J.H.F., Lavin, Y., Lau, C.M., Goloborodko, A., Feng, J., Fujisaki, J., Ding, L., et al. (2016). Hematopoietic stem cells are the major source of multilineage hematopoiesis in adult animals. *Immunity* 45, 597–609.
- Serup, P., Gustavsen, C., Klein, T., Potter, L.A., Lin, R., Mullapudi, N., Wandzioch, E., Hines, A., Davis, A., Bruun, C., et al. (2012). Partial promoter substitutions generating transcriptional sentinels of diverse signaling pathways in embryonic stem cells and mice. *Dis. Model. Mech.* 5, 956–966.
- Sun, J., Ramos, A., Chapman, B., Johnnidis, J.B., Le, L., Ho, Y.J., Klein, A., Hofmann, O., and Camargo, F.D. (2014). Clonal dynamics of native hematopoiesis. *Nature* 514, 322–327.
- Tsang, J.C., Yu, Y., Burke, S., Buettner, F., Wang, C., Kolodziejczyk, A.A., Teichmann, S.A., Lu, L., and Liu, P. (2015). Single-cell transcriptomic

- reconstruction reveals cell cycle and multi-lineage differentiation defects in Bcl11a-deficient hematopoietic stem cells. *Genome Biol.* 16, 178.
- Wilson, A., Laurenti, E., Oser, G., van der Wath, R.C., Blanco-Bose, W., Jaworski, M., Offner, S., Dunant, C.F., Eshkind, L., Bockamp, E., et al. (2008). Hematopoietic stem cells reversibly switch from dormancy to self-renewal during homeostasis and repair. *Cell* 135, 1118–1129.
- Wilson, N.K., Kent, D.G., Buettner, F., Shehata, M., Macaulay, I.C., Calero-Nieto, F.J., Sánchez Castillo, M., Odekeven, C.A., Diamanti, E., Schulte, R., et al. (2015). Combined single-cell functional and gene expression analysis resolves heterogeneity within stem cell populations. *Cell Stem Cell* 16, 712–724.
- Yang, G., Xu, Y., Chen, X., and Hu, G. (2007). IFITM1 plays an essential role in the antiproliferative action of interferon-gamma. *Oncogene* 26, 594–603.
- Yu, V.W.C., Yusuf, R.Z., Oki, T., Wu, J., Saez, B., Wang, X., Cook, C., Barayawno, N., Ziller, M.J., Lee, E., et al. (2016). Epigenetic Memory Underlies Cell-Autonomous Heterogeneous Behavior of Hematopoietic Stem Cells. *Cell* 167, 1310–1322.e17.